American Journal of Materials Science 2019, 9(2): 36-43
DOI: 10.5923/j.materials.20190902.02

Metal Injection Molding for Production of Biodegradable Implants: An Analysis of the Potential of Pure Iron for Application in Stents

A. C. Tavares[1], P. Mariot[2], L. L. Costa[3,*], L. Schaeffer[4]

[1]Mechanical Manufacturing Technologist, Federal University of Rio Grande do Sul (UFRGS), Brazil
[2]Materials Engineer, Professor at University of Vale do Itajaí (Univali), Itajaí (SC), Brazil
[3]Mechanical Engineer, Federal University of Rio Grande do Sul (UFRGS), Porto Alegre (RS), Brazil
[4]Mechanical Engineer, Professor at Federal University of Rio Grande do Sul (UFRGS), Porto Alegre (RS), Brazil

Abstract Powder injection molding is an advanced process technique of powder metallurgy that allows the production of parts with complex geometries with no need of workmanship, high productivity, series production of parts and uniform microstructure. In the present study, injectable mixtures were characterized and their applicability in the production of endovascular orthoses was tested. The volumetric fraction of metallic powder in the injection mixture, sintering temperature, porosity volume, mechanical and surface properties of pure iron samples obtained by IMP were determined. It was observed that the production of injectable mixtures above the critical volume can introduce interesting properties as a larger over compared as other samples, which remained below the critical content of powder obtained by injection molding present superior properties to the pure iron of Fusion. It was developed a new appliance for the injection molding process (IMP) added to the use of pure iron as biodegradable metal with potential for application in stents.

Keywords Powder injection molding, Powder metallurgy, Endovascular orthoses, Pure iron samples

1. Introduction

The process currently utilized for the manufacture of precursor tubes for application in stents of bioinert materials is complex and involves several steps. The current production flow promotes high inherent cost and results in material ductility loss.

Previous studies have shown that the injection molding process (IMP) process is suitable for the manufacture of small and complex parts that require porosity degree control through the production parameters [1].

The first parameter to be controlled in the production of thin-walled metallic components through IMP is particle size. Previous studies have shown that to obtain thin wall components (100-400 m), it should be used the average particle size up to 5 m, equiaxial and predominantly rounded [2]. Furthermore, mean particle sizes above a critical value result in dimensional quality and surface roughness of the "green" and sintered samples deterioration, this fact is not interesting in implants.

* Corresponding author:
luana.lucca@ufrgs.br (L. L. Costa)
Published online at http://journal.sapub.org/materials

The particle size distribution also influences the densification achieved, the sintering process and the metal powder mixing process efficiency, which is another important factor in obtaining thin walls. The agglutinating system promotes injection mass fluidity, facilitating the path within the mold cavity. Thus, the use of a large particle size distribution curve results in increased densification, reducing the minimum amount of polymeric binders required in the injection mixture [3]. These factors directly influence the injectable mixture viscosity.

Studies relating IMP with the use of pure iron with biomedical application are rare. A crucial factor for this study is the sintering temperature determination that directly influences the mechanical properties of yield (Re), mechanical strength (Rm) and elongation. Studies have shown that temperature influences the increase of pore volume in a sintered material and porosity in a biodegradable implant is beneficial for vascularization and consequently for biocompatibility [4].

In IMP produced materials, it is not uncommon for the porosity distribution to be heterogeneous. In this case, the localized deformation will occur preferentially in regions with punctual pores concentration. The pores reduce the area of the effective section and act as locations of stress concentration for localized deformation, reducing both mechanical resistance and ductility [5-8].

Materials for application to stents must be allied with mechanical resistance and ductility to withstand the tensions generated by the blood vessel, allowing the balloon expansion [9,10] and resisting the pressure applied by the catheter balloon between 5 and 7 atm (0.6 MPa) with radial forces that reach values between 18 and 21 N. Another mechanical property that should be considered is the elongation, between 30 and 50% of elongation until the material fracture, the flow curve being of extreme importance for the analysis [11,12]. Iron in other studies has already shown adequate radial strength due to its high modulus of elasticity. This feature makes it a mechanically viable option to obtain structures with thin walls (100 to 300 m) [12].

This study aims to employ and develop the IMP of stents using pure iron as a biodegradable metal. The studies of the properties of injectable mixtures carried out herein are to verify whether it is the product of the injection of metal powders for the production of metallic enamel prostheses, verifying whether the produced loads would have the capacity of injection in the thickness of the walls of stents and if the mechanical properties of the stents injected test bodies.

2. Materials and Methods

Pure iron was supplied by the manufacturer Sintez ® . The impurities maximum degree of the iron powder used was of 0.02% ℃ and 0.26% ℃ as analyzed by the manufacturer. The morphology was observed using a scanning electron microscope(SEM), model JEOL® 6060, using a voltage of 20 kV.

The granulometric distribution determination was performed using Malvern Mastersizer X laser diffraction granulometer in aqueous medium. The critical metal volume was determined using a method according to the procedure described by Kong [13]. A Haake Rheomix 3000P® rheometer with blade rotors with a Rheocord Haake 252 module was used for the test. The test temperature was 175℃ with a constant rotation of 40 rpm. The metal powder is added to the stepwise mixture in the amount of 1% (volume) for each step, from 60% to 63%. The torque variations as a function of time were monitored during the test duration.

The differential scanning calorimetry (DSC) test was carried out with the main objective of characterizing as injection mixtures in relation to the melting temperature and homogeneity. A TA Instruments® , model Q-600 with argon protective atmosphere, was used in a continuous flow of 50 mL / min. The sample mass was between 5.8 and 7.2mg.

The heating rate used in the test was 10℃/min and the final temperature was 850℃. This temperature range comprises the meltdown and degradation transformations temperatures of the injection mixtures polymers analyzed. For the injection molding step success, it is necessary to characterize the shear rate effect on the viscosity of the injection mixture at a given temperature. The rheological behavior of the mixtures studied injection was determined using a capillary rheometer counter, model Ceast Smart Rheo 2000® , according to ASTM D3835. The apparent viscosity as a function of the shear rate was automatically calculated by the equipment program. A commercial composition using AISI 8620 steel powder was used as a control sample, since it is known that this composition has as characteristic, the high drop in viscosity with the shear rate increase, that is, high pseudoplasticity. The injection mixture ideal composition determination used for the manufacture of test specimens for tensile testing was performed in two steps. The first one had as objective to evaluate the different constituent polymer components effect of the binder system in the filling of a test-mold. The injection mixtures compositions evaluated in this step are given in Table 1.

Table 1. Different injection mixtures' compositions used in the rheological test

	% volumetric				
Component	1	2	3	4	Commercially available
Metal Powder	62	62	62	62	~ 61-63
PP	17,4	-	-	-	-
PEBD	-	-	21,0	17	-
PEAD	-	20,5		-	-
Carnauba	-	-	13.3	-	-
Parafina	19,3	16,5	2,5	19,5	~ 12-17
PMMA	-	-	-	-	~15-20
Estearic Acid	1,3	1,0	1,2	1,5	~1.5

The second step, with the best mixture composition already determined, sought to evaluate the increase effect of the metallic powder volume fraction on the final properties studied throughout the present research. The compositions used in this step are shown in Table 2.

Table 2. Composition of the samples' injection mixtures produced

Component	Volume (%)			
Pure iron	54	58	62	66
Polipropileno (PP)	19,7	18,7	17,7	16,9
Parafina	19,3	18,5	18,0	17,5
Esteáric Acid	3,0	2,8	2,3	1,9

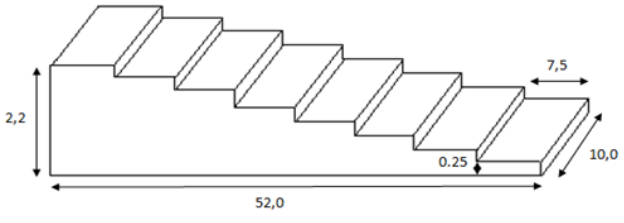

Figure 1. Dimensional diagram of the test body for evaluation of mold filling. Measurements in millimeters

In order to characterize the injectable mixtures behavior during the injection molding stage, mainly the mold filling capacity for different mixtures, a mold was used as shown in Figure 1.

This sample geometry is not described in official standards, but its use for mold fill study has been described previously [14]. The test mold complete filling allows to predict that the injection mixture has viscosity low enough to fill cavities of the order of 250 m (Figure 2), i.e., the approximate wall thickness of a tube for application in stents [12]. The injection molding was performed using an Arburg 170S injector with closing capacity of 170 kN and Battenfeld 300 with 300 kN of closing capacity.

The samples obtained by injection have the dog bone shape, with a nominal length of 95mm and a test section of 15.6 mm^2. The binder system extraction was carried out with a stage of thermal extraction preceded by chemical extraction by immersion in hexane. The immersion time in hexane was 4 h at 60°C degrees. The thermal extraction stage had slow heating to avoid defects from hydrocarbon migration in its gaseous form to the material surface. The sintering of all test specimens was carried out in a reducing atmosphere consisting of a mixture of gases composed of H2 (2%) and Ar (98%). The heating rate was 0.5°C/min to the temperature of 450°C for the thermal extraction of the binder and pre-sintering. This rate is considerably low for thermal extraction patterns of parts usually produced by IMP, but its use is aimed at minimizing the retention of organic material in the sintered samples. The residence time at 450°C was 60 min.

A heating rate of 5°C/min was used up to the sintering temperature, followed by cooling at 10°C/min in reducing atmosphere to room temperature. Three different sintering temperatures were used: 1040, 1080 and 1120°C, to evaluate the sintering temperature effect on the sintered material properties. The maximum temperature plateau was maintained for 30min. For each volumetric fraction of metallic powder used (54, 58, 62 and 66% vol.) There are 3 sintering temperatures. To facilitate the understanding, from this step, the samples containing volumetric fraction of metallic powder equal to 54% and sintered at 1040°C were identified throughout the text as "54/1040" and so on for the others. The sintered samples density was determined using the immersion method (Archimedes Principle) according to ASTM B-311. This method was also used to measure the biomaterials density with porosity percentages between 4 [15] and 30% [16]. Five samples of each condition were used to ensure the results reliability.

For the metallographic assay, parts were cut from traction samples in square prisms of dimensions 0.8 x 4 x 4 mm. Subsequently the parts were sanded and polished to a surface finish of 0.3 m. The etching was done with dilute nitric acid (3%) for metallography and the characterization was performed under an optical microscope (Leica DFC-320).

3. Results

The iron powder morphology used to obtain the samples is shown in Figure 2. The particles have a regular spherical morphology, and they are considered ideal for the IMP process.

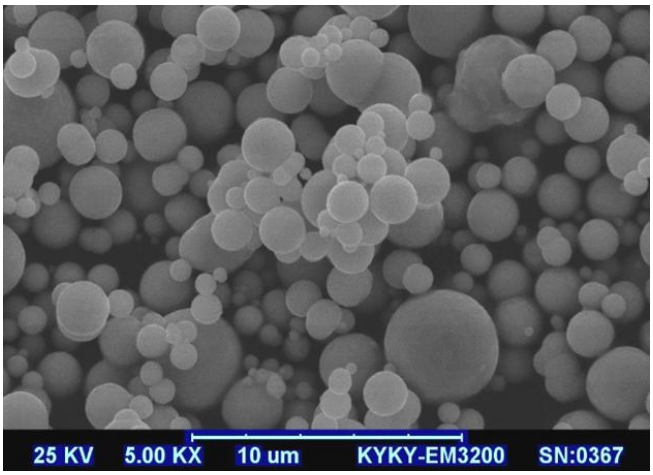

Figure 2. Iron powder morphology used (SEM)

The pure iron powder particles granulometric distribution is shown in Figure 3. The sample shows a wide distribution of particle sizes and monomodal shape. The monomodal distribution does not contribute to the packing between the metallic powder particles, resulting in a lower sintered material densification when compared to bimodal distributions. The average particle diameter found (d50) was 3.48 μm.

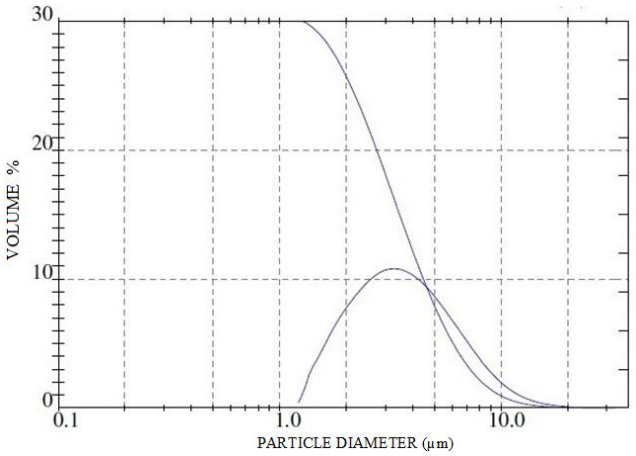

Figure 3. Pure Fe particle size distribution

The calorimetric curves for the different injection mixtures, whose compositions were shown in Table 1, are shown in Figure 4.

In Figure 4, calorimetric curve of the studied mixtures made it possible to determine the melting (between 120.7 and 154.7°C) and constituent polymers degradation temperatures (between 459.7 and 484.1°C). Endothermic peaks characterize the paraffin wax melting in each blend,

the structural polymer melt temperature range, and the peak relative to the paraffin wax degradation and structural polymer degradation of each composition. However, mixture 3 (Table 1) showed poorly defined endothermic peaks, which may be associated with heterogeneities resulting from low mixing efficiency (Supati et al., 2000). Mixture 1 showed well defined endothermic peaks, indicating high homogeneity achieved during the mixing step. Figure 5 shows the shear rate influence (1/s) on the apparent viscosity (Pa.s), measured in capillary rheometer.

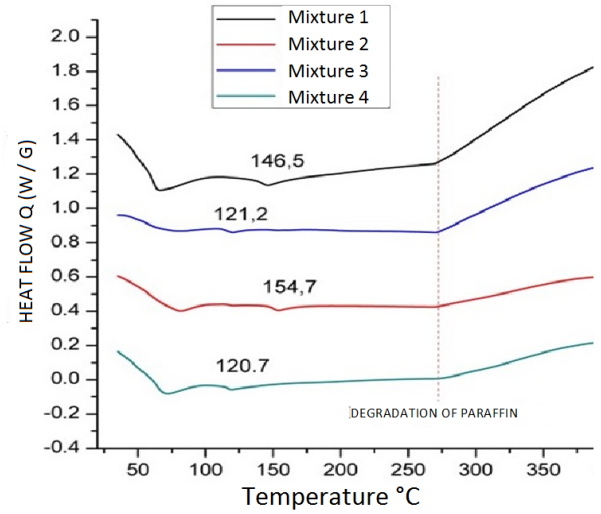

Figure 4. Calorimetric curves of the studied mixtures

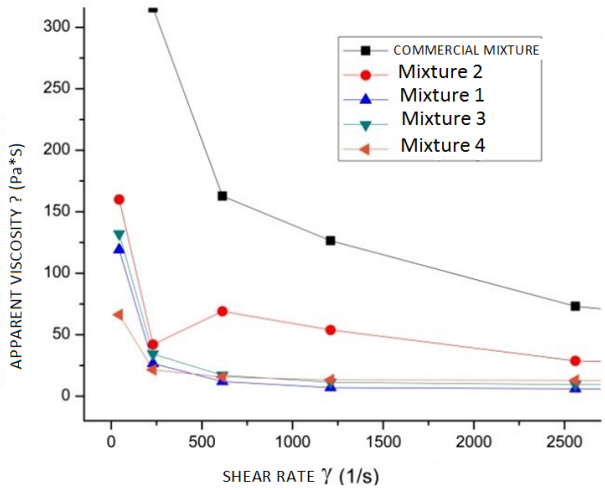

Figure 5. Shear rate influence, (1/s) on the apparent viscosity (Pa.s) of the injectable mixtures compositions studied. The assay temperature was 160℃

All the different mixtures showed a drop in apparent viscosity with the increase of applied shear rate, mainly up to 250 1/s, that is the behavior of non-Newtonian fluid of the pseudoplastic type. Mixture 2 presented an anomalous behavior to the value of 500 [1/s], which is possibly due to micro heterogeneities in the injection mixture. As expected, the commercial composition presented levels of higher viscosity as a function of the shear rate compared to the other compositions. The samples shaped according to the injection parameters of Table 4 are shown in Figure 6.

Figure 6. Molded samples for mold fill evaluation

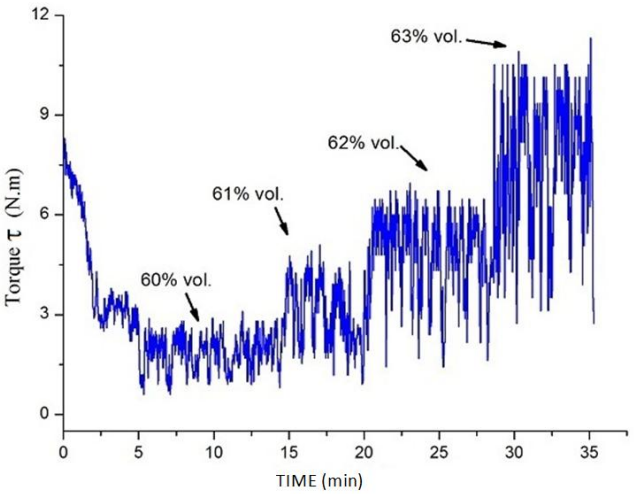

Figure 7. Time-based mixing torque for pure iron volumetric fractions of 60, 61, 62 and 63%

Mixtures of numbers 2 and 3 showed insufficient mold filling (arrows). The injection parameters as pressure and temperature were kept constant for the four different mixtures studied. Figure 6 shows the samples after the molding step (green parts). The samples made from the blend 4 exhibited dimensional deformation at the thinner end. This phenomenon is not associated with defects of the injection molding stage, but with the rapid cooling from the mold extraction, whose temperature was maintained at 70℃. Considering the mold filling, the mixture 1, whose thermoplastic polymer is polypropylene, (Table 1) presented better performance when compared with the others. This composition presented the best combination of properties (Figures 5, 6 and 7) for the injection molding of thin wall parts and was selected for continuity of the pure iron sample manufacturing process for the subsequent tests. Figure 7 shows the mixing torque versus time for various volumetric

fractions, using the polymers of blend 1 as the basis. At each point where the powder was added to the mixture, the torque showed a start and then the reach of a state of relative stability, associated with the homogenization of the same. As reported in previous studies once the critical metal volume is exceeded, excessive loading causes the mixture to exhibit instability [17].

In this test the critical metallic volume was 63%, since this percentage resulted in the greatest magnitude between the variations in torque. To achieve high densification in the sintered parts, a metallic volume slightly lower than the critical volume should be used. For this reason, one of the compositions evaluated in this study has a metallic powder volume fraction of 62% (Table 2). Once the best composition among the blends evaluated was defined, the next step was the samples injection that were used for the mechanical, physical and surface tests. Figure 8 shows the test samples compared to green and after the sintering, the green parts did not present defects from the injection step and sintering stage, such as dimensional distortions or surface oxidation, it is still possible to observe the length of the samples.

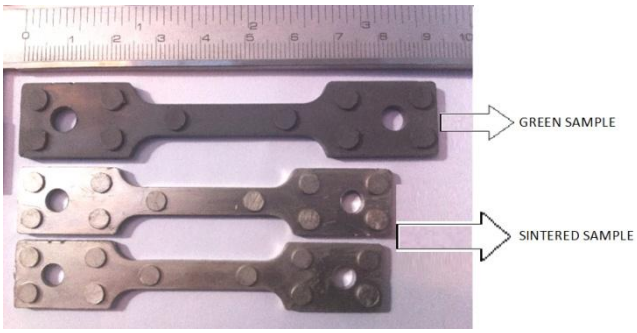

Figure 8. Samples in the "green" and sintered state, showing the volumetric contraction caused by sintering

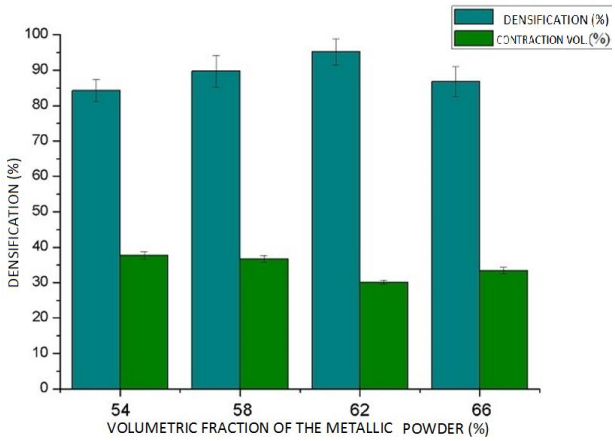

Figure 9. Volumetric densification and retraction as a function of the volumetric fraction of pure iron powder

Figure 9 shows the relative density (in percent) as a function of the metallic powder volumetric fraction used in the injection mixture. For the results shown in this figure, the sintering temperature of 1080℃ was used. It is observed that the metallic powder volumetric fraction increase leads to the samples densification increase up to the metallic fraction value of 62%. In addition, the samples showed volumetric contraction decrease with the metallic powder fraction increase up to the value of 62%, corresponding to the increase in the densification.

The density in the samples sintered state with iron volumetric fraction equal to 62% is approximately 95% of the theoretical density, which presented the highest densification among all samples studied. The samples containing 66% of metallic powder in the injection mixture showed lower densification than those containing 62%. The iron samples porous structure prepared from the injection mixtures containing metallic powder volumetric fraction between 54 and 66% is shown in Figure 11. The sintering temperature for these samples was 1080℃, with the objective of evaluating the metal fraction variation effect. For comparison, Figure 11e shows the pure iron sample porous microstructure obtained by melting, which contains homogeneously distributed fine pores.

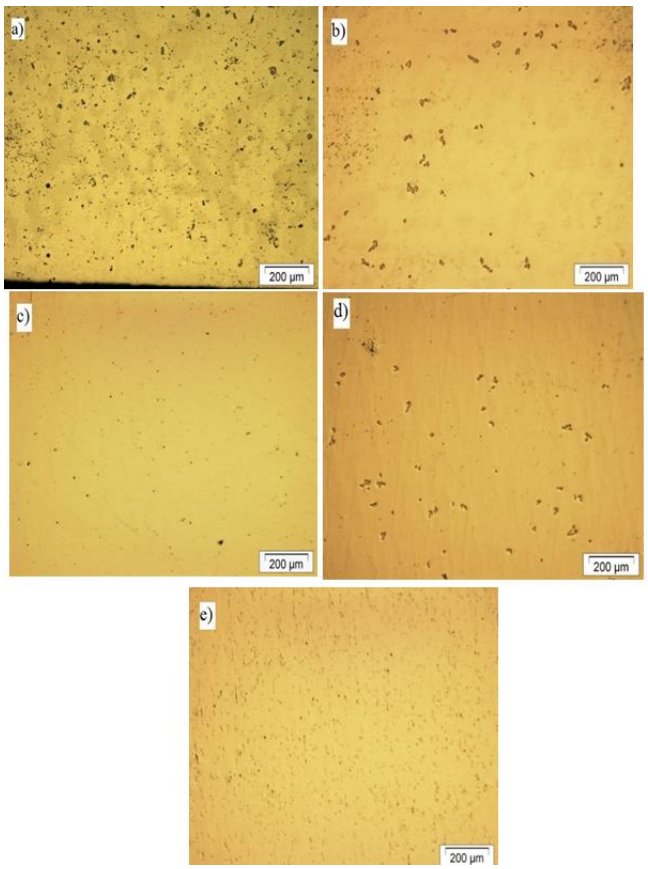

Figure 10. Sintered pure iron containing volumetric fraction (initially in the injection mixture) of (A) 54, (b) 58, (c) 62, (d) 66%, sintered at 1080℃ and (e) pure iron manufactured by fusion

While sample 54/1080 (Figure 10a) showed an irregular distribution of pore sizes and high degree of porosity, samples 66/1120 (Figure 10d) have on average a larger pore size, a more regular distribution of pore sizes and a region between larger and more densified pores. The other samples had intermediate microstructures. The sample containing 62% of metallic powder (Figure 10c) showed the smallest pore sizes between the samples obtained by IMP and large

regions between pores, confirming the densification values presented in Figure 10. This structure was achieved due to the value of 62% be close to the critical volumetric fraction (63%) for the samples studied. While samples containing 62% of metal fraction showed smaller pores, the samples containing 66% had coalesced pores and greater space between pores.

Samples containing 66% of metallic fraction showed pores of irregular morphology when compared to the others, particularly when compared to the sample containing 62%, also showing a certain amount of angular pores. The sample containing 54% iron powder has a higher degree of porosity than the sample containing 66%. The iron samples microstructures prepared from the injection mixtures containing volumetric fraction of metallic powder of 54% and sintered at 1040, 1080 and 1120℃ are shown in Figure 11.

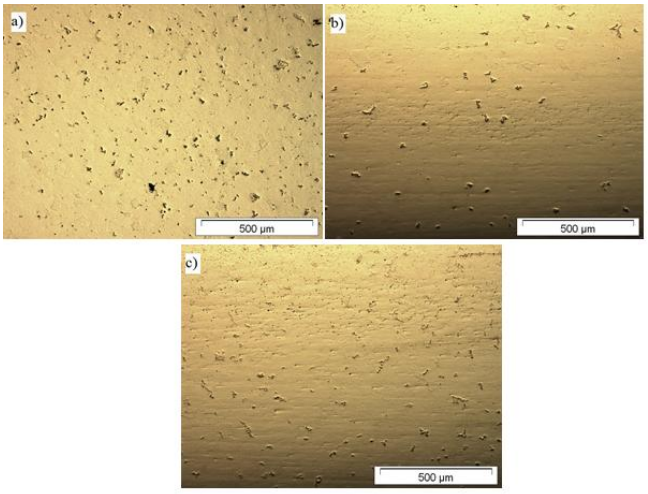

Figure 11. Sintered pure iron containing volumetric fraction (initially in the injection mixture) of 54% and sintered at (a) 1040, (b) 1080 and (c) 1120℃

The samples with the smallest volumetric fraction were chosen due to the relatively high porosity level, allowing to indicate specifically the effect of the sintering temperature on the pore structure. As expected, the increase in the sintering temperature leads to a decrease in porosity and a decrease in pore size. While the sample sintered at 1040℃ shows an irregular distribution of pore size, samples sintered at 1080 and 1120℃ have a large number of small pores, with larger pores distributed and a larger pore region. Figure 12 shows the sintered samples microstructure at 1080℃ and with metallic powder volumetric fraction between 54 and 66%. The pure iron obtained by melting was used for comparison (Figure 12e).

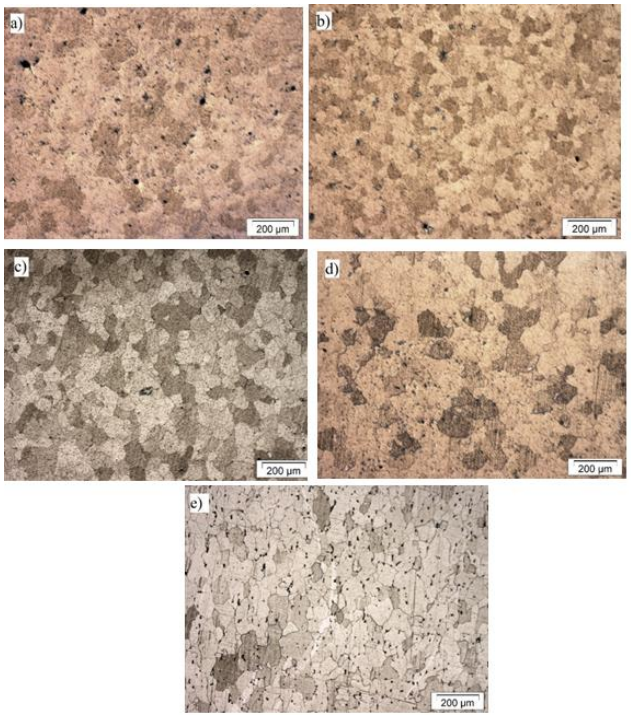

Figure 12. Sintered samples microstructure at 1080℃ and with metallic powder volumetric fraction between (A) 54%, (b) 58%, (c) 62%, (d) 66% and (e) pure iron produced by melting

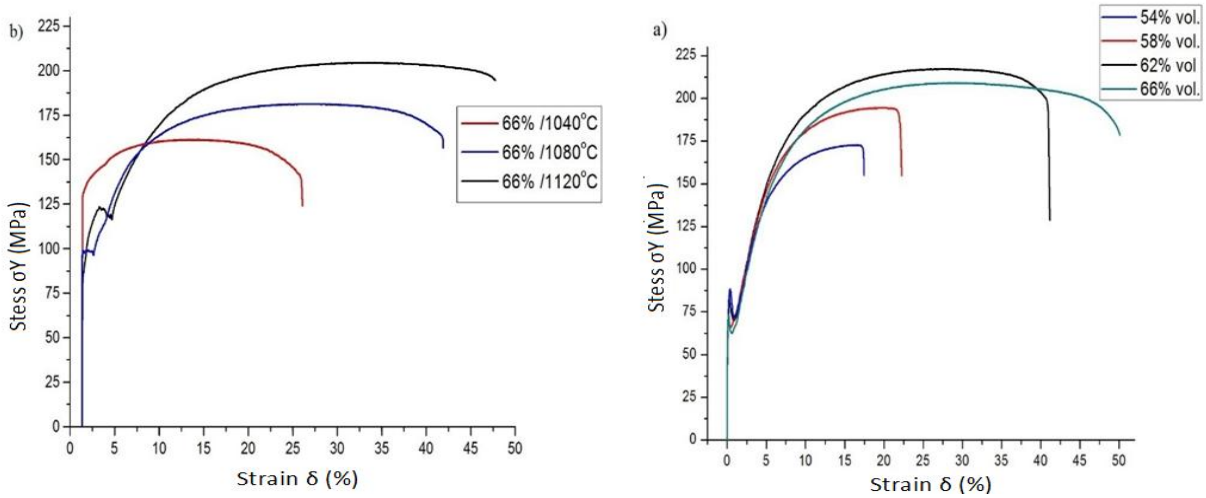

Figure 13. Samples tensile-strain diagrams: (A) with different volumetric fractions of metallic powder and sintered at 1120℃ and (b) with a fraction of 66% and sintered at different temperatures

The sample containing 66% metallic powder initially in the injection mixture showed higher grain size compared to the other samples. The samples micrographs with metallic volumetric fractions equal to 54, 58 and 66% show that the samples surface preparation was not efficient, resulting in slightly unfocused micrographs with a great number of scratches. But grain outlines are visible. There was no significant difference between the mean grain sizes between the samples containing 54, 58 and 62% of metallic powder. There is also no significant difference compared to the sample obtained by melting.

Figure 13 shows the engineering tensile-strain diagram (l / 100 x 100) of sintered pure iron with different metallic volumetric fractions, sintered at 1120℃ (Figure 13a) and containing 66% by volume of pure iron sintered at different temperatures (Figure 13b). The mechanical properties are shown in Table 3.

Figure 13b shows the samples mechanical behavior containing 66% of the volumetric fraction in pure iron powder and sintered at different temperatures. In general, the pure iron volumetric fraction increase, as expected, results in the increase in the maximum limit of mechanical resistance. With the metallic volumetric fraction decrease, the elongation until the fracture drastically reduces. The mechanical behavior of the samples was significantly consistent with the pore structures variation shown in Figure 10. The pore volume decreased with the increase in the volumetric fraction of powder between 54 and 62% and then increased. As the porosity had a direct influence on the mechanical strength, the flow limit increased from 59 MPa (54%) to 87 MPa (62%) and the resistance limit of the sample containing 62% of iron powder reached the maximum value, since the resistance to deformation increased with decreasing porosity. The iron powder volumetric fraction increasing from 62 to 66% resulted in a resistance limit decrease (Figure 14a). The modulus of elasticity, or Young's modulus of the pure iron samples studied, as well as other mechanical properties, are shown in Table 3.

Table 3. Samples mechanical properties with different metallic powder volumetric fractions and different sintering temperatures

Condition	Re (MPa)	E (GPa)	Elongation (%)
54 %/1040℃	59±5	90	13
54 %/1080℃	-	-	-
54 %/1120℃	86 ±3	101	17.3
58 %/1040℃	73 ±4	95	10
58 %/1080℃	84 ±3	100	24.5
58 %/1120℃	85 ±2	105	22.2
62 %/1040℃	96 ±5	91	12
62 %/1080℃	139 ±5	165	16
62 %/1120℃	87 ±4	178	40.8
66 %/1040℃	128 ±5	110	26.4
66 %/1080℃	100 ±4	128	42.5
66 %/1120℃	114 ±3	110	50

Comparing the mechanical behavior of these two samples, the 66% sample showed a greater elongation until fracture (50%) than the sample with 62% (41%).

In general, with higher sintering temperatures, the pores amount decreased, requiring a greater energy amount for the elastic deformation. For comparison, Song et al. (2014) found a Young's modulus of 205 GPa for pure cast iron and 190 GPa for 316-L stainless steel. Banerjee et al. (2013) found 110 GPa for titanium and Bowen et al. (2013) reported a Young's modulus of 44 GPa with deformation up to 13% fracture for a magnesium alloy with potential application for biodegradable stent.

4. Conclusions

Exceeding the critical metal powder volumetric fraction (63%) resulted in a more irregular distribution of pores with a larger average size, as compared to the sample of metallic volumetric fraction close to the critical value. When the volumetric fraction of metallic powder exceeds the critical value, the amount of polymeric binder is not sufficient to fill the space between all the particles. As a result, void spaces may be formed in the injection mixture.

Clearly, the increase in the sintering temperature leads to an increase in the resistance limit. This can be explained by the samples greater densification. The increase in densification resulted in an increase in the resistance limit. The maximum deformation until fracture also increased from 26.4 to 50%, as the sintering temperature increased from 1040 to 1120℃.

The pure iron manufactured by IMP showed exceptionally high ductility (from 13 to 50% deformation to fracture) while the mechanical strength was between that of magnesium alloys and stainless steel AISI 316-L. Interestingly, the sintered samples which injection mixture contained a 66% of metallic powder volumetric fraction (above the critical fraction) presented the greatest deformation until fracture.

REFERENCES

[1] K. Nishiyabu et al, Micro metal injection molding using hybrid micro/nano powders, Materials Science Forum. 534-536 (2007) 381-384.

[2] K. Kim et al, Fabrication and material properties of powder injection molded Fe sintered bodies using nano Fe powder, Materials Letters. 61 (2007) 1218-1222.

[3] TAKEKAWA, J., Effect of binder composition on debinding and sintering processes of injection molded Fe-8Ni mixed powders, Journal of Materials Research. 11 (1997) 512-520.

[4] M. Wolf et al. Benefits and limitations of biodegradable Mg implants and parts, produced by Metal Injection Moulding, European Cells and Materials. 28 (2014) 12-20.

[5] A. Hadrboletz, B Weiss, Fatigue behavior of iron based

sintered material: A review. International Materials Review. 42 (1997) 1-44.

[6] X. Deng et al, Fatigue crack growth behavior of hybrid and prealloyed sintered steels Part I. Microstructure characterization, Materials Science and Engineering. 491 (2008) 19-27.

[7] N. Chawla, X. Deng, Microstructure and mechanical behavior of porous sintered steels, Materials Science and Engineering. 390 (2005) 98-112.

[8] H. Housseini et al, Effect of Pore Characteristics on Mechanical Properties of Highly Porous NiTi Shape Memory Alloys, The International Conference on Shape Memory and Superelastic Technologies (SMST). (2013) 324-325.

[9] F. Li et al, Simulation of the grain structure evolution of a Mg-Al-Ca-based alloy during hot extrusion using the cellular automation method, Key Engineering Materials. 491 (2012) 265-272.

[10] S. Garg, W. Patrick, M. Serryus, Coronary Stents - Current Status, Journal of the American College of Cardiology. 56 (2010) 10.

[11] A.P.G Nogueira, Desenvolvimento de método para medição de força radial em endopróteses aórticas [Dissertation]. Porto Alegre (2011).

[12] H. Hermman, D. Mantovani, Process of prototyping coronary stents from biodegradable Fe-Mn alloys, Acta Biomaterialia. 9 (2013) 8585-8592.

[13] X. Kong, T. Barriere, J.C. Gelin, Determination of critical and optimal powder loadings for 316L fine stainless steel feedstocks for micro-powder injection molding, Journal of Materials Processing Technology. 212 (2012) 2173-2182.

[14] M. Wright, L.J. Hughes, S.H. Gressel, Rheological characterization of feedstocks for metal injection molding, Journal of Materials Engineering and Performace. 3 (1994) 301-306.

[15] F. Kafkas, T. Ebel, Metallurgical and mechanical properties of Ti–24Nb–4Zr–8Sn alloy fabricated by metal injection molding, Journal of Alloys and Compounds, 617 (2014) 359-366.

[16] G. Chen, NiTi alloys produced by press-and-sinter from Ni/Ti and Ni/TiH2 mixtures, Materials Science and Engineering. 582 (2013) 117-125.

[17] N.H. Supati, K.A. Loh, S.B. Thor, Mixing and characterization of feedstock for powder injection molding, Materials Letters. 46 (2000) 109-114.